Research Article | Vol. 25, No. 5 | 6 Mar 2017 | OPTICS EXPRESS 5044

Optics EXPRESS

Frequency- and time-domain nonlinear distortion compensation in high-speed OFDM-IMDD LR-PON with high loss budget

HSING-YU CHEN,[1,3] CHIA-CHIEN WEI,[2,*] CHE-YU LIN,[1] LI-WEI CHEN,[1] I-CHENG LU,[1,3] AND JYEHONG CHEN[1]

[1]*Department of Photonics, National Chiao-Tung University, Hsinchu 300 Taiwan*
[2] *Department of Photonics, National Sun Yat-sen University, Kaohsiung 804 Taiwan*
[3]*Information and Communications Research Labs, Industrial Technology Research Institute, Hsinchu 310, Taiwan*
ccwei@mail.nsysu.edu.tw

Abstract: This study compared two nonlinear distortion compensation techniques, SSII cancellation (in the frequency domain) and Volterra filtering (in the time domain), in a >50-Gbps/λ OFDM-IMDD LR-PON. Experiment results for SNR, BER, and data rate (based on a bit-loading algorithm) revealed that the performance of frequency-domain SSII cancellation is unaffected by power fading; however, it depends heavily on the precision of the mathematical model. Conversely, although time-domain Volterra filtering is affected by the faded waveform, adaptive-weighting provides flexibility in dealing with mixed nonlinear distortion, particularly that associated with the interplay between fiber dispersion and fiber nonlinearity. 4-channel WDM-OFDM and 3rd-order Volterra filtering were used to demonstrate the feasibility of the proposed scheme in a 200-Gbps IMDD system. Based on 10-GHz EAM and PIN, we achieved 200-Gbps transmission over a distance of 60 km with a loss budget of >30 dB, while providing support for 128 ONUs at >1.6 Gbps/ONU without the need for an inline amplifier or pre-amplifier.

OCIS codes: (060.2330) Fiber optics communications; (060.0060) Fiber optics and optical communications.

References and links

1. Cisco, "The Zettabyte Era—Trends and Analysis," *http://www.cisco.com/c/en/us/solutions/collateral/service-provider/visual-networking-index-vni/VNI_Hyperconnectivity_WP.html*, (2015).
2. K.-I. Suzuki, M. Fujiwara, T. Imai, N. Yoshimoto, and H. Hadama, "128 x 8 split and 60 km Long-reach PON Transmission using 27 dB-gain hybrid burst-mode optical fiber amplifier and commercial giga-bit PON system," in *Proceedings of Optical Fiber Communication Conference*, (2010), paper NWB3.
3. D. Z. Hsu, C.-C. Wei, H.-Y. Chen, J. Chen, M. C. Yuang, S. H. Lin, and W. Y. Li, "21 Gb/s after 100 km OFDM long-reach PON transmission using a cost-effective electro-absorption modulator," Opt. Express **18**(26), 27758–27763 (2010).
4. ITUT G.989.1, "40-Gigabit-capable passive optical networks (NG-PON2): General requirements," (2013).
5. N. Cvijetic and M. Cvijetic, "What is Next for DSP-based Optical Access and OFDMA-PON?" in *Proceedings of European Conference on Optical Communication* (2014), pp. 1–3.
6. D. Shea and J. Mitchell, "A 10 Gb/s 1024-way-split 100-km long-reach optical-access network," J. Lightwave Technol. **25**(3), 658–693 (2007).
7. D. Z. Hsu, C. C. Wei, H. Y. Chen, Y. C. Lu, and J. Chen, "A 40-Gbps OFDM LR-PON system over 100-km fiber employing an economical 10-GHz-based transceiver," in *Proceedings of Optical Fiber Communication Conference*, (2012), paper OW4B.2.
8. C. Cole, I. Lyubomirsky, A. Ghiasi, and V. Telang, "Higher-order modulation for client optics," IEEE Commun. Mag. **51**(3), 50–57 (2013).
9. K. Zhong, X. Zhou, T. Gui, L. Tao, Y. Gao, W. Chen, J. Man, L. Zeng, A. P. T. Lau, and C. Lu,"Experimenal study of PAM-4, CAP-16, and DMT for 100 Gb/s short reach optical transmission systems," Opt. Express **23**(2), 1176–1189 (2015).
10. FSAN, "FSAN Highlights & NG-PON2 Standards Update," in *Proceedings of FSAN and IEEE NG-EPON/1904 ANWG Joint Session* (2015).
11. H.-Y. Chen, C.-C. Wei, I. C. Lu, Y.-C. Chen, H.-H. Chu, and J. Chen, "EAM-based high-speed 100-km OFDM transmission featuring tolerant modulator operation enabled using SSII cancellation," Opt. Express **22**(12), 14637–14645 (2014).

#283006 https://doi.org/10.1364/OE.25.005044
Journal © 2017 Received 15 Dec 2016; revised 17 Feb 2017; accepted 20 Feb 2017; published 24 Feb 2017

Optics EXPRESS

12. H. Y. Chen, C.-C. Wei, I.-C. Lu, H.-H. Chu, Y.-C. Chen, and J. Chen, "High-Capacity and High-Loss-Budget OFDM Long-Reach PON Without an Optical Amplifier [Invited]," J. Opt. Commun. Netw. **7**(1), A59–A65 (2015).
13. C.-C. Wei, H.-Y. Chen, H.-H. Chu, Y.-C. Chen, C.-Y. Song, I.-C. Lu, and J. Chen, "32-dB loss budget high-capacity OFDM long-reach PON over 60-km transmission without optical amplifier," in *Proceedings of Optical Fiber Communication Conference* (2014), paper Th3G.1.
14. W. Yan, B. Liu, L. Li, Z. Tao, T. Takahara, and J. C. Rasmussen, "Nonlinear distortion and DSP-based Compensation in Metro and Access Networks using Discrete Multi-tone," in *Proceedings of European Conference on Optical Communication* (2012), paper Mo.1.B.2.
15. H. Y. Chen, C. C. Wei, C. Y. Lin, L. W. Chen, I. C. Lu, and J. Chen, "A 200-Gbps OFDM long-reach PON over 60-km transmission without inline and pre-amplifier," in *Proceedings of Optical Fiber Communication Conference*, (2015), paper Th1H.2.
16. C. C. Wei, H. L. Chen, H. Y. Chen, Y. C. Chen, H. H. Chu, K. C. Chang, I. C. Lu, and J. Chen, "Analysis of nonlinear distortion and SSII cancellation in EAM-Based IMDD OFDM transmission," J. Lightwave Technol. **33**(14), 3069–3082 (2015).
17. J. Tsimbinos and K. V. Lever, "Computational complexity of Volterra based nonlinear compensators," Electron. Lett. **32**(9), 852–854 (1996).
18. T. N. Duong, N. Genay, M. Ouzzif, J. Le Masson, B. Charbonnier, P. Chanclou, and J. C. Simon, "Adaptive loading algorithm implemented in AMOOFDM for NG-PON system integrating cost-effective and low-bandwidth optical devices," IEEE Photonics Technol. Lett. **21**(12), 790–792 (2009).

1. Introduction

According to a report published by Cisco [1], metro traffic had surpassed long-haul traffic by 2014. Furthermore, metro traffic is expected to continue growing at double the rate of long-haul traffic until at least 2019. This can be attributed primarily to rapid growth in the number of mobile devices and a change in the habits of users leading to increased internet activity. These changes have gradually shifted the bandwidth bottleneck to metro systems and the last-mile. Long-reach (LR) passive optical networks (PON) are viewed as promising candidates for the next-generation passive optical network 2 (NG-PON2) standard [2–4]. Several transmission techniques have been developed to improve data rates and satisfy the coverage of LR-PON, including orthogonal frequency-division multiplexing (OFDM), wavelength-division multiplexing (WDM) and coherent detection [5]. Despite the superior performance of coherent detection, the intensity modulation and direct detection (IMDD) scheme is still preferred for access networks due to its low cost [6,7]. High-order modulation (HOM) is viewed as a high bandwidth efficiency format suitable for the most cost-sensitive client optics [8]. In [9], it was revealed that 100-Gbps PAM-4 (pulse amplitude modulation), CAP-16 (carrier-less amplitude and phase modulation), and OFDM in a short-reach system provide nearly the same receiver sensitivity, but OFDM imposes less computational complexity. Furthermore, the use of 10G-class components and the IMDD scheme makes it possible for OFDM to achieve data rates of ≥ 40 Gbps with a reach of ≥ 60 km. This has made OFDM LR-PON one of the more promising candidates for the development of low-cost, high-capacity access networks with wide coverage. The WDM technique has also been considered for the NG-PON2 standard to fulfill demand for network traffic while providing a seamless bridge to future-proof networks [10].

Nonetheless, several issues continue to hinder the transmission performance of OFDM-IMDD LR systems, such as modulator nonlinearity, transmission-induced nonlinear distortion, dispersion-induced power fading, and low loss budget [11–13]. Increasing fiber launch power to enable self-phase modulation (SPM) has been proposed as a means to improve transmission bandwidth while increasing the loss budget [12,13]. Unfortunately, high fiber launch power induces high fiber nonlinearity, which essentially cancels out any benefits provided by the enhanced bandwidth, and may actually result in lower data rates. A 2nd-order model based on an electro-absorption modulator (EAM), which is referred to as subcarrier-to-subcarrier intermixing interference (SSII), has been proposed to provide compensation for nonlinear distortion [11–13]. Based on the SSII model, a corresponding SSII cancellation technique has also been developed to compensate for nonlinear distortion in the frequency domain at receiver side. Compensation for nonlinear distortion can also be

Optics EXPRESS

applied in the time domain, using the well-known Volterra filtering technique [14,15]. The received waveform is modeled as a 2nd or higher order Volterra series in order to apply compensation at receiver side by calculating weighting values for each term in the series.

In this work, we compare SSII cancellation against Volterra filtering at receiver side in a single-channel experiment using various configurations involving various fiber launch powers. The signal-to-noise ratio (SNR), bit error rate (BER), and data rates (based on a bit-loading algorithm) were used to analyze the performance and limitations of each method. We then constructed a 4-channel WDM-OFDM to demonstrate the feasibility of the proposed schemes in a 200-Gbps 60-km OFDM-IMDD system. Experiment results demonstrate that the application of high fiber launch power in conjunction with compensation for nonlinear distortion can reduce the variations in performance between channels by 18%. Based on 10-GHz EAM and PIN, we achieved 200-Gbps transmission over a distance of 60 km with loss budget of >30 dB, while providing support for 128 ONUs at >1.6 Gbps/ONU without the need for an inline amplifier or pre-amplifier.

2. Theory of nonlinear compensation

2.1 SSII cancellation

EAM-based transmission can be represented as a 2nd-order model. The optical power generated by a nonlinear EAM can be approximated as $P \cong P_B(1+X+p_2X^2)$, where P_B is the DC power, $X = X(t) = \sum_{n=1}^{N} \Re\{x_n e^{jn\omega t}\}$ is the normalized AC power envelop, x_n is the quadrature amplitude modulation (QAM) symbol encoded on the n^{th} subcarrier, N is the number of subcarriers, $\omega/(2\pi)$ is the subcarrier spacing, and p_2 is the weighting of nonlinearity in the 2nd-order modulator. The measured chirp parameter of the EAM is almost entirely a linear function of bias, so the chirp parameter α can be represented as $\alpha \cong \alpha_0 + \alpha_1 X$, where the α_0 and α_1 depend on the bias voltage [16]. Thus, the envelop of the chirped optical field can be written as $E = \sqrt{P}\exp(-j(\alpha/2)\ln P)$. Increasing fiber launch power increases the effect of SPM. However, the complex nonlinear Schrödinger equation is required to solve for the SPM effect precisely. For the sake of simplicity, the SPM effect was decoupled from dispersion in [11,12], to approximate the overall SPM-induced nonlinear phase shift as $\Phi_{\mathrm{NL}} \cong \gamma L_{\mathrm{eff}} P$, where γ is the fiber nonlinear coefficient, and L_{eff} is the effective fiber length. Thus, the normalized optical field with the SPM is $\bar{E} = E \times \exp(j\Phi_{\mathrm{NL}})/\sqrt{P_B}$, and its 2nd-order approximation is as follows:

$$\bar{E} \cong e^{j\phi_{\mathrm{NL}}} \times \left[1 + \frac{\sqrt{1+\alpha_{eff,0}^2}}{2} e^{-j\theta_\alpha} X - \frac{(1+\alpha_{\mathrm{eff},0}^2 - 4p_2) + j2(\alpha_{\mathrm{eff},1} + 2\alpha_{\mathrm{eff},0}p_2)}{8} X^2\right] \quad (1)$$

where $\theta_\alpha = \tan^{-1}(\alpha_{eff,0})$, $\alpha_{\mathrm{eff},0} = \alpha_0 - 2\phi_{\mathrm{NL}}$, and $\alpha_{\mathrm{eff},1} = \alpha_1 - 2\phi_{\mathrm{NL}}$. Decoupled dispersion is then seen to create parabolic phase shifts in each frequency component. Let $\Theta\{\cdot\}$ represent the effect of dispersion transmission. It follows $\Theta\{X\} = \Sigma_{n=1}^{N} \Re\{x_n e^{jn\omega t}\} \cdot e^{jn^2\theta_D}$ because chromatic dispersion induces the phase shift of $n^2 \times \theta_D = n^2 \times \omega_s^2 \beta_2 L/2$ for the n^{th} subcarriers in both optical sidebands, where L and β_2 are the fiber length and dispersion parameter, respectively. Then, the received signal after square-law photo-detection is $I_{ph} = |\Theta\{\bar{E}\}|^2$, and its 2nd-order approximation is as follows:

Optics EXPRESS

$$I_{ph} \cong 1+\sqrt{1+\alpha_{\text{eff},0}^2}\cdot X\cos(n^2\theta_D-\theta_\alpha)+\underbrace{\frac{1+\alpha_{\text{eff},0}^2}{4}\left[\left|\Theta\{X\}\right|^2-\mu\cdot\Re\left\{\Theta\{X^2\}e^{j\theta_p}\right\}\right]}_{\text{SSII}} \quad (2)$$

where, $\theta_p=\tan^{-1}\left(2(\alpha_{\text{eff},1}+2\alpha_{\text{eff},0}p_2)/(1+\alpha_{\text{eff},0}^2-4p_2)\right)$, and $\mu=\left[1-4p_2/(1+\alpha_{\text{eff},0}^2)\right]\cdot\sec\theta_p$. The 1st and 2nd term of I_{ph} represent the DC signal and the desired OFDM signal, respectively. The cosine in the 2nd term determines the frequency-selective power fading, which is affected by $\alpha_{eff,0}$. The 3rd term in Eq. (2) is SSII or the mixed 2nd-order distortion contributed by the dispersion, modulator nonlinearity, chirp, and SPM effect. Following the estimation of θ_p and μ using training symbols, the standard decision results of OFDM subcarriers are regarded as X in the calculation of SSII in accordance with Eq. (2). The resulting SSII is then used to compensate for mixed nonlinear distortion associated with SSII cancellation.

2.2 Volterra filtering

Unlike frequency-domain SSII cancellation, Volterra filtering is a nonlinear compensation scheme operating in the time domain [14,15]. Based on the Volterra series, the m^{th} sample of the output signal after the nonlinear filter is

$$y(\mathrm{m})=\sum_{l_1=0}^{N_v-1}w_1(\mathrm{l}_1)\,\mathrm{r}(\mathrm{m}-\mathrm{l}_1)+\sum_{l_1=0}^{N_v-1}\sum_{l_2=0}^{N_v-1}w_2(\mathrm{l}_1,\mathrm{l}_2)\prod_{i=1}^{2}\mathrm{r}(\mathrm{m}-\mathrm{l}_i)+\sum_{l_1=0}^{N_v-1}\sum_{l_2=0}^{N_v-1}\cdots\sum_{l_k=0}^{N_v-1}w_k(\mathrm{l}_1,\mathrm{l}_2,\ldots,\mathrm{l}_k)\prod_{i=1}^{k}\mathrm{r}(\mathrm{m}-\mathrm{l}_i) \quad (3)$$

where $\mathrm{r}(\mathrm{m}-\mathrm{l}_i)$ is the $(\mathrm{m}-\mathrm{l}_i)^{\text{th}}$ sample of the received signal, $w_k(\mathrm{l}_1,\mathrm{l}_2,\ldots,\mathrm{l}_k)$ is the weighting factor of the k^{th} order, and N_v is the memory length. The 1st term in Eq. (3) represents a linear filter, whereas the others are nonlinear. Taking a larger number of nonlinear terms into consideration may lead to better performance; however, this would dramatically increase the computational complexity. To limit the computational complexity of Volterra filtering, we considered two cases: the application of 2nd- and 3rd-order Volterra filtering while disregarding nonlinear terms higher than the 2nd- and 3rd-order, respectively. To reduce complexity, only the 3rd-order terms of $\mathrm{l}_1=\mathrm{l}_2=\mathrm{l}_3$ are included in the 3rd-order filtering, such that the added complexity of the 3rd-order terms is linearly proportional to N_v. Unlike SSII cancellation, Volterra filtering does not require a detailed model of nonlinearities. The key to Volterra filtering involves identifying the optimal weighting factors, which can be obtained using the Wiener solution: $\mathbf{w}=\mathbf{R}^{-1}\mathbf{p}$, where $\mathbf{w}$ is the column vector composed of all weighting factors under consideration. Let $\mathbf{r}$ represent the column vector composed of linear and nonlinear input signals (i.e. $\{\prod_{i=1}^{k}\mathrm{r}(\mathrm{m}-\mathrm{l}_i)\}_{k=1}^{2\text{ or }3}$) corresponding to those in $\mathbf{w}$. $\mathbf{R}=E[\mathbf{r}\mathbf{r}^{\mathrm{T}}]$ is the signal correlation matrix, and $\mathbf{p}=E[\mathrm{d}(\mathrm{m})\mathbf{r}]$ is the cross-correlation vector between the desired and input signals ($\mathrm{d}(\mathrm{m})$ and $\mathbf{r}$), where $E[\cdot]$ is the expectation value. We use the sample mean to replace the expectation value in finding $\mathbf{w}$ using training symbols.

Optics EXPRESS

3. Single-channel experiment setup and results

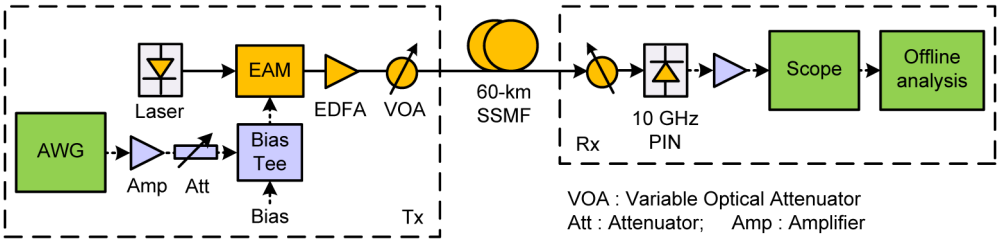

Fig. 1. Experiment setup of EAM-based OFDM-IMDD 60-km transmission.

Figure 1 presents the experiment setup used in this study. The baseband electrical OFDM signal was generated by an arbitrary waveform generator (AWG, Tektronix AWG70002A), featuring a sampling rate of 50-GS/s and 8-bit resolution. The driving signal consisted of a 16-QAM OFDM signal with FFT size of 1024 and a CP of 16, and the data were encoded at the 2nd–227th subcarriers with a bandwidth of 10.5 GHz. An electrical attenuator (preceded by an electrical amplifier) was inserted to adjust the driving power of the EAM (CIP 10G-LR-EAM-1550). A DFB laser was modulated externally using an OFDM-driving EAM, followed by an Erbium-doped fiber amplifier (EDFA) and a variable optical attenuator (VOA) to achieve launch power of 6–18 dBm. After standard single-mode fiber (SSMF) transmission over a distance of 60 km, the signal was direct-detected using a 10-GHz PIN receiver and captured using a digital oscilloscope (Tektronix DPO 71254) at a sampling rate of 50 GS/s and 3-dB bandwidth of 12 GHz. The captured digital signal was demodulated using an offline DSP program, which applied either SSII cancellation or Volterra filtering. Finally, the SNR was measured and the number of errors was determined in order to calculate the BER.

To compensate for nonlinear distortion in the OFDM-IMDD system, we respectively employed SSII cancellation and Volterra filtering. There are two main differences between these two compensation methods. First, SSII cancellation is applied in the frequency domain, whereas Volterra filtering is applied in the time domain. Second, SSII cancellation involves the calculation of interference based on the mathematical model in Eq. (2), whereas Volterra filtering involves the adaptive calculation of weighting factors based on a comparison of transmitted and received waveforms. Thus, Volterra filtering does not require the precise transmission model used in SSII cancellation. Nonetheless, dispersion-induced power fading results in the destruction of part of the waveform, degrades the accuracy of Volterra filtering, and increases noise through equalization. Moreover, the complexity of a 2nd-order SSII cancellation is briefly $O(N_s \cdot \log(N_s))$ [16], where N_s is the FFT size. For a 2nd-order Volterra filtering, the number of operation of an N_v taps filter for each symbol is briefly $N_s \cdot (N_v + N_v^2)$ [17]. Therefore, the complexity of a 2nd-order Volterra filtering can be represent as $O(N_s \cdot N_v^2)$. Besides, since the 3rd-order terms in the 3rd-order filtering include only those of $l_1 = l_2 = l_3$ in Eq. (3), the complexities of the 2nd- and 3rd-order filtering are similar. Thus, the complexity of 2nd-order Volterra filtering is higher than SSII cancellation in our case.

Optics EXPRESS

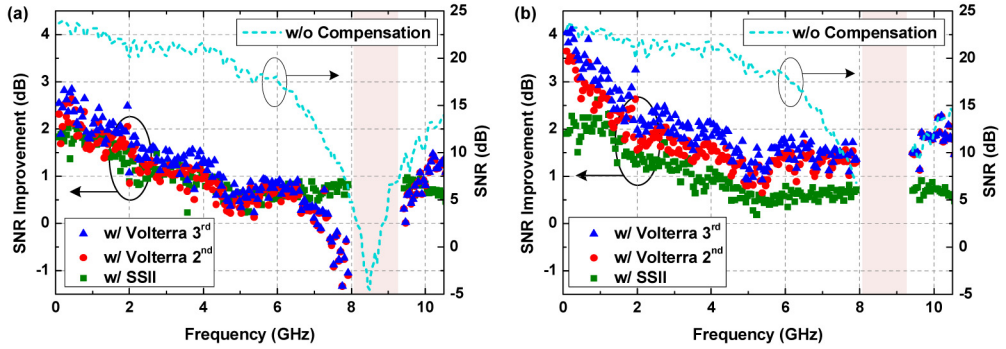

Fig. 2. SNR at 60 km and corresponding improvements obtained using various compensation methods: (a) prior to removal of any subcarriers and (b) following removal of 30 faded subcarriers.

Figures 2(a) and 2(b) show the SNR and the corresponding improvements obtained using the two methods after transmission over a distance of 60 km, with the fiber launch power set to 6 dBm and the received power set to –8 dBm. In Fig. 2(a), every subcarrier within 10.5 GHz is utilized. Regardless of the nonlinear distortion, the dispersion-induced power fading dominates the performance around the frequency of 8.5 GHz, which can be observed from the SNR. As one would expect, Volterra filtering is not as effective as SSII cancellation with regard to improving SNR. Furthermore, the SNR of some subcarriers actually drops after employing Volterra filtering. In contrast, hard decisions are performed before calculating SSII, thereby avoiding noise enhancement and penalty in SNR. Fortunately, the performance of Volterra filtering can be improved by operating each subcarrier of the OFDM signal independently, thereby enabling the removal of faded subcarriers prior to transmission. In Fig. 2(b), 30 subcarriers (164th to 193th) in the region with severe power fading are removed at the transmitter. When Volterra filtering is applied, all of the remaining subcarriers show improvements in SNR without any penalty. In contrast, SSII cancellation (in the frequency domain) is unaffected by faded subcarriers, such that the SNR of each subcarrier remains nearly the same.

We selected the aggregate data rate to facilitate a performance comparison of the two compensation methods. The aggregate data rate was estimated from the SNR of each subcarrier using the bit-loading algorithm at a target BER of 3.8×10^{-3} (7% FEC overhead) [18]. Figures 3(a) and 3(b) present the data rate as a function of the number of subcarriers removed using SSII cancellation, 2nd-, or 3rd- order Volterra filtering. Note that only the subcarriers with the most severe fading were removed. More precisely, a certain number of carriers centered at the dip of channel frequency response were removed. In Fig. 3(a), EAM is operated in a relatively linear region, using a bias of –0.75 V. Without removing any subcarriers, the data rate of the signal with SSII cancellation was superior to that obtained using Volterra filtering. When applying either 2nd- or 3rd-order Volterra filtering, an increase in the number of removed subcarriers led to a sharp increase in the data rate. This is because the removal of faded subcarriers eliminated the issue of noise enhancement in Volterra filtering. Furthermore, 3rd-order Volterra filtering slightly outperformed 2nd-order Volterra filtering, thanks to the partial compensation afforded by 3rd-order nonlinearity. Similar to the SNR results in Figs. 2(a) and 2(b), the data rate is insensitive to the removal of subcarriers when SSII cancellation is applied. In Fig. 3(b), the bias was set to –0.95 V, which is a highly nonlinear region. We observed trends similar to those in Fig. 3(a); however, SSII cancellation outperformed 2nd-order Volterra filtering in this configuration. This can be attributed to the enhancement of high-order (>2nd-order) nonlinear distortion by the Volterra filtering under these bias conditions. Model-based SSII cancellation is unaffected by this issue due to the hard decisions made prior to SSII calculation. In addition, the data rate benefited from

Optics EXPRESS

negative chirp enhanced bandwidth [11]. This is a clear demonstration that operating settings must be optimized for each method in order to achieve the best data rate.

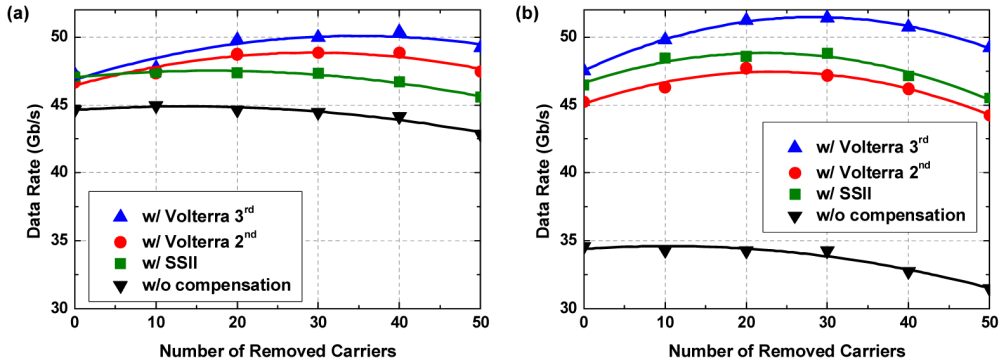

Fig. 3. Data rate as a function of the number of removed subcarriers at EAM bias voltages of (a) –0.75 and (b) –0.95 V.

The SPM effect can be used to compensate for dispersion-induced power fading, resulting in a dramatic improvement in transmission bandwidth to over 10 GHz [12,13]. In Fig. 4, the fiber launch power was set to 18 dBm in order to generate pronounced SPM effects, thereby moving the faded dip to beyond 10.5 GHz. However, the SNR values in Fig. 4 are far lower than those in Figs. 2(a) and 2(b), due to the distortion induced by fiber nonlinearity. As shown in Fig. 4, after eliminating mixed nonlinear distortion, all of the compensation methods produced a considerable improvement in SNR. The elimination of a faded dip within the signal bandwidth eliminates the need to remove any subcarriers at the transmitter when applying Volterra filtering. The highest SNR improvement of 12.7 dB was achieved when 3rd-order Volterra filtering was applied. Nonetheless, rather than calculating the complicated nonlinear Schrödinger equation, SSII cancellation is based on simplified assumptions pertaining to SPM effects. This oversimplified model makes SSII cancellation to underperform 2nd-order Volterra filtering at 9–10.5 GHz, as shown in Fig. 4.

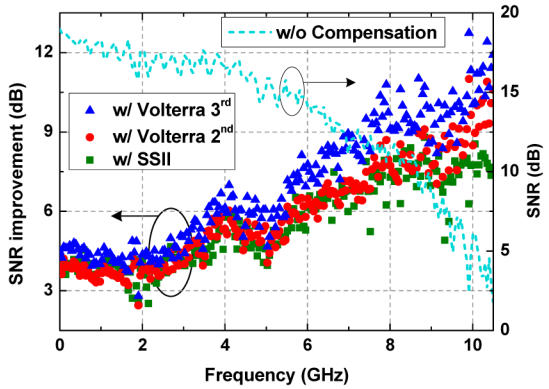

Fig. 4. SNR improvement using fiber launch power of 18 dBm and various compensation schemes.

Optics EXPRESS

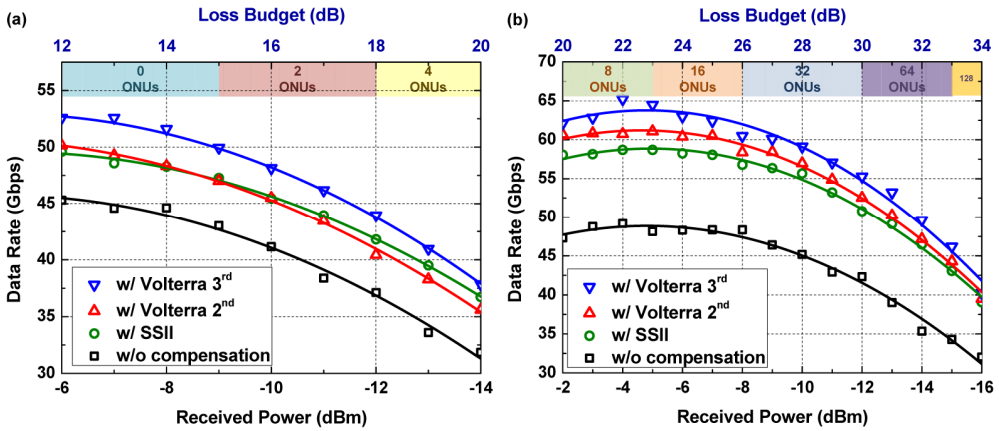

Fig. 5. Estimated data rate at each received power with fiber launch set to (a) 6 dBm and (b) 18 dBm.

To analyze the performance of SSII cancellation and Volterra filtering in a more systematic manner, we formulated Figs. 5(a) and 5(b) to summarize the estimated data rate versus the received power using individually optimized driving power and bias voltage. In accordance with the analysis in Fig. 3, we removed 30–40 subcarriers at the transmitter in order to preserve the compensation capacity of Volterra filtering, as shown in Fig. 5(a). The number of the removed subcarriers depends on the optimized condition at each received power. For example, at the received power of −8 dBm, the highest data rate is achieved at the bias of −0.95 V with 40 removed subcarriers, as show in Fig. 3. Figure 5 also shows the loss budget, which equals the launch power minus the received power, which is provided as a reference. The data rates in Fig. 5(a) were measured under a normal launch power of 6 dBm. Under these conditions, the system was unable to achieve a data rate of 50 Gbps prior to the application of any compensation method. Each of the compensation methods lowered the minimum received power required to attain a data rate of 50 Gbps as follows: SSII cancellation (−6 dBm), 2nd- Volterra filtering (−6 dBm), and 3rd-order Volterra filtering (−8.9 dBm). SSII cancellation and 2nd-order Volterra filtering achieved essentially the same performance, which is a clear indication that the SSII model provides sufficient precision within this configuration. However, the loss budget of a 50-Gbps transmission under these conditions was less than 15 dB. Considering the 12-dB loss associated with 60-km SSMF and the 3K-dB loss for power sharing among 2^K ONUs, a loss budget capable of supporting only 2 ONUs is unacceptable for an LR-PON.

The method used to increase the fiber launch power (Fig. 4) can be used to improve the transmission bandwidth as well as increase the loss budget. Figure 5(b) presents the data rates obtained when using launch power of 18 dBm. Prior to the application of compensation, the data rate was limited by mixed nonlinear distortion. The application of SSII cancellation, 2nd-, and 3rd-order Volterra filtering lowered the minimum received power required to achieve a data rate of 50 Gbps to below −12 dBm. This means that the proposed system is able to provide a loss budget of >30 dB while providing support for 64 ONUs. However, the SSII model is based on the oversimplified assumption of high fiber launch power transmission. As a result, 2nd-order Volterra filtering outperforms SSII cancellation, as shown in Fig. 5(b). Overall, these results demonstrate that a 64-ONU 50-Gbps OFDM-IMDD LR-PON can be achieved using any of the three compensation methods.

Optics EXPRESS

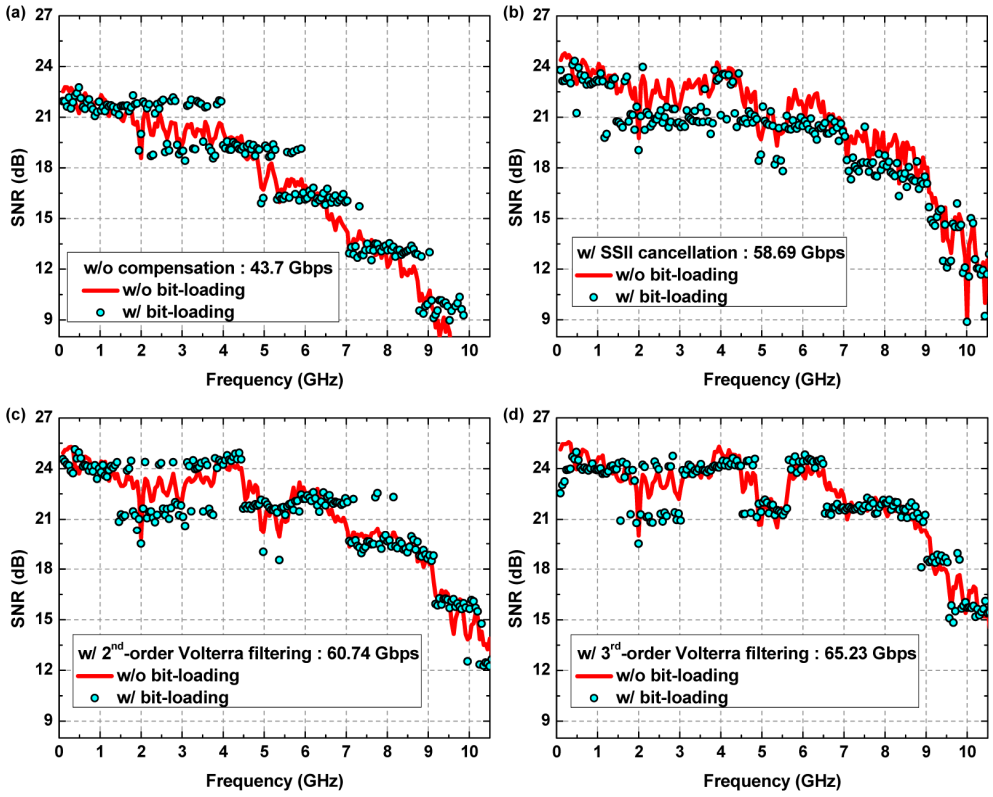

Fig. 6. SNR values with and without the application of the bit-loading algorithm: (a) without compensation; (b) SSII cancellation; (c) 2nd-order Volterra filtering; and (d) 3rd-order Volterra filtering.

To confirm the estimated data rates in Fig. 5, we chose the settings used for the highest data rate in Fig. 5(b); i.e., the conditions for the 3rd-order Volterra filtering at a received power of –4 dBm. Under these settings, the achievable data rates were as follows: without compensation (43.7 Gbps), SSII cancellation (58.7 Gbps), 2nd- Volterra filtering (60.7 Gbps), and 3rd-order Volterra filtering (65.2 Gbps). The corresponding SNR values of the subcarriers with and without the application of the bit-loading algorithm are presented in Figs. 6(a)–6(d). The measured BERs in Figs. 6(a) (2.1×10^{-3}), 6(b) (2.8×10^{-3}), 6(c) (2.4×10^{-3}), and 6(d) (3.2×10^{-3}) are all below the FEC limit (BER = 3.8×10^{-3}), thereby confirming the estimated results in Fig. 5. In addition, the corresponding 64- and 128-QAM constellations of the 65.23-Gbps signal in Fig. 6(d) while employing different compensation schemes are shown in Fig. 7. The improvement of constellations' quality can be clearly observed after employing nonlinear distortion methods.

Optics EXPRESS

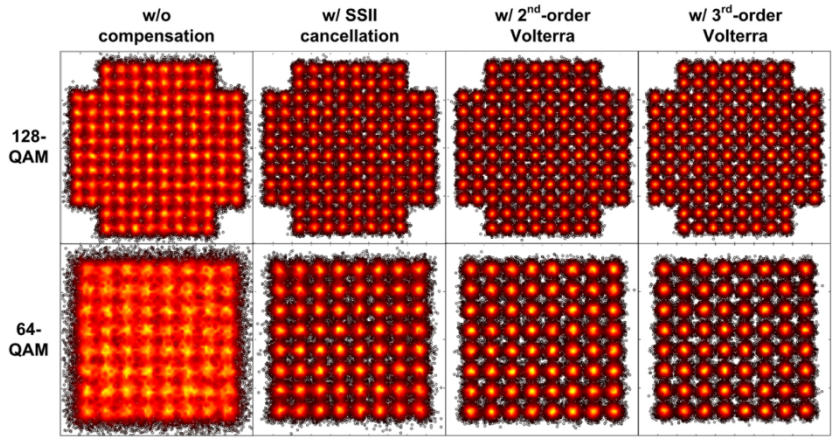

Fig. 7. The corresponding 64- and 128-QAM constellations of the 65.23-Gbps signal in Fig. 6(d) while employing different compensation schemes.

4. Multi-channel experiment: Setup and results

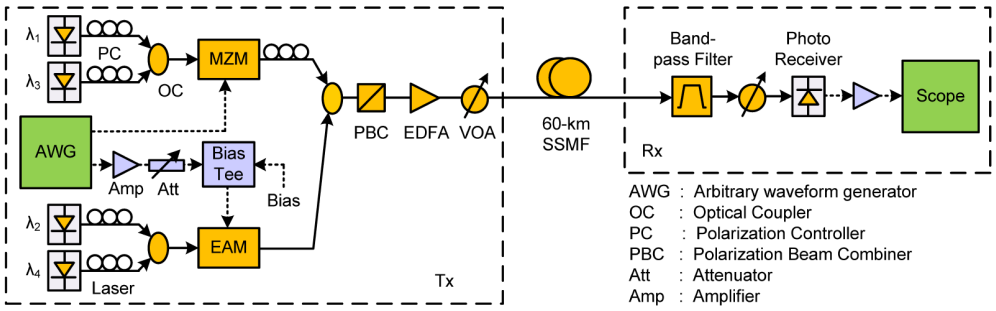

Fig. 8. Experiment setup of 4-channel WDM-OFDM transmission system.

We used 4-channel OFDM transmission to demonstrate the feasibility of the proposed scheme in a WDM system. Figure 8 illustrates the experiment setup of the 4-channel system using a signal with the same 10.5-GHz bandwidth. Four DFB lasers with wavelength of 5-nm spacing were used as light sources in the WDM-OFDM system. Wavelength λ_1 of 1545.57 nm and λ_3 of 1555.57 nm were modulated using a 10-GHz Mach-Zehnder modulator (MZM), and wavelength λ_2 of 1550.57 nm and λ_4 of 1550.57 nm were modulated using a 10-GHz EAM. Due to the lack of another EAM, we used MZM to emulate odd channels. After measuring λ_1 and λ_3, the wavelength pairs of EAM and MZM were swapped to measure λ_2 and λ_4. To demonstrate the worst case involving the most pronounced inter-channel interference, we combined the channels using an optical coupler (OC), followed by a polarizer to ensure that all WDM channels were co-polarized. A gain-flattened EDFA and VOA were then used to achieve a total launch power of 13–24 dBm. Figure 9 resents the optical spectrum at the output of the EDFA at a resolution of 0.1 nm. After SSMF transmission over a distance of 60 km, a band-pass filter (BPF) was used to emulate a typical 4-channel WDM demultiplexer. The signal of each channel was then detected directly using a 10-GHz PIN and demodulated using an off-line DSP program.

Optics EXPRESS

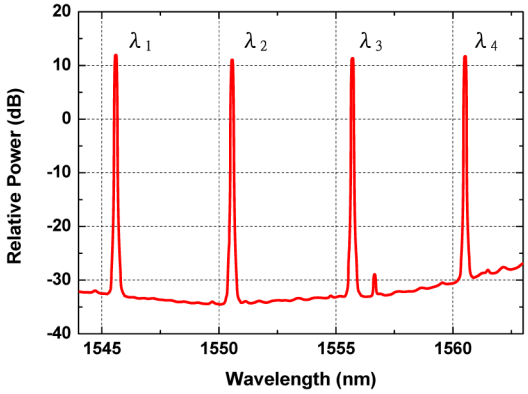

Fig. 9. Optical spectrum after EDFA.

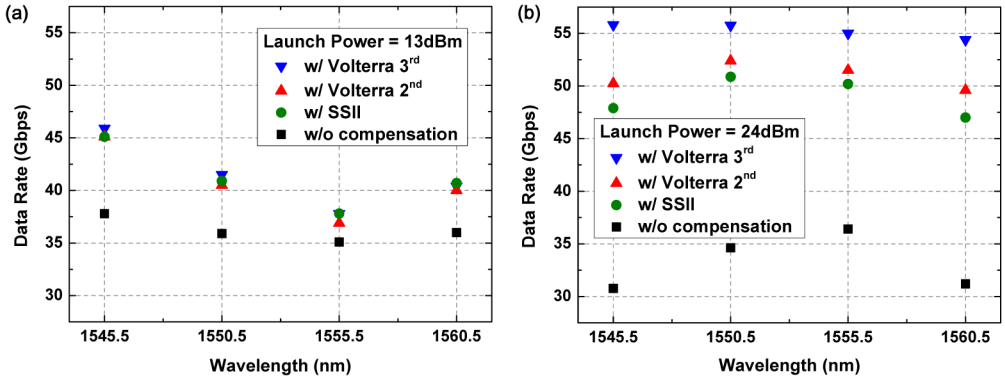

Fig. 10. Estimated data rates at each wavelength using the proposed compensation methods under fiber launch power of (a) 13 dBm and (b) 24 dBm.

Figure 10 presents the data rate estimated for each channel at a received power of –9 dBm. As in the single-channel experiment, the bias and driving voltage were individually optimized for each wavelength. In Fig. 10(a), the total fiber launch power was set to 13 dBm (i.e. 7 dBm/λ). As in the single-channel results, the signal suffered from power fading. As a result, the 2nd- and 3rd- order Volterra filtering resulted in similar performance. As shown in Fig. 10(b), increasing the total fiber launch power to 24 dBm (i.e. 18-dBm/λ) made it possible for 2nd-order Volterra filtering to outperform SSII cancellation in every channel. Furthermore, each of the compensation schemes attained huge improvements through the elimination of nonlinear distortion. Figures 11(a) and 11(b) present the SNR values corresponding to the configurations using 3rd-order Volterra filtering respectively shown in Figs. 10(a) and 10(b). In Fig. 11(a), the difference in fading at different wavelengths was caused by dispersion as well as wavelength- and bias- dependent chirp [14]. The differences in response produced large variations in the data rates at the various wavelengths, thereby increasing the complexity of the system design. The difference in data rates reached 21% (i.e., 37.8 Gbps at λ_3 and 45.9 Gbps at λ_1). Figure 11(b) shows the SNR when the fiber launch power was increased to 18 dBm for each channel. Fading dip in each channel increased to beyond 10.5 GHz thanks to the considerable effects of SPM, which resulted in a channel response smoother than that obtained under normal launch power. This reduced the difference in SNR values and moderated the variations in data rates at the various wavelengths, thereby lowering the maximum difference in data rate to only 3% (55.8 and 54.4 Gbps), representing a reduction of 18%.

Optics EXPRESS

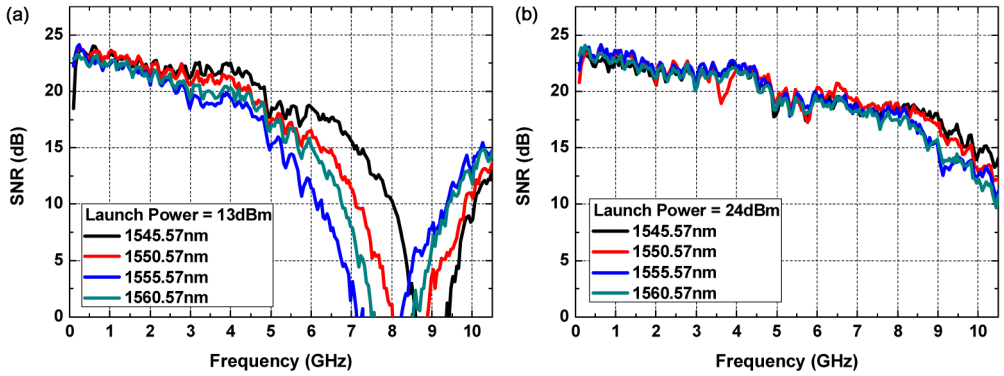

Fig. 11. SNR of each subcarrier at each wavelength using 3rd-order Volterra filtering under fiber launch power of (a) 13 dBm and (b) 24 dBm.

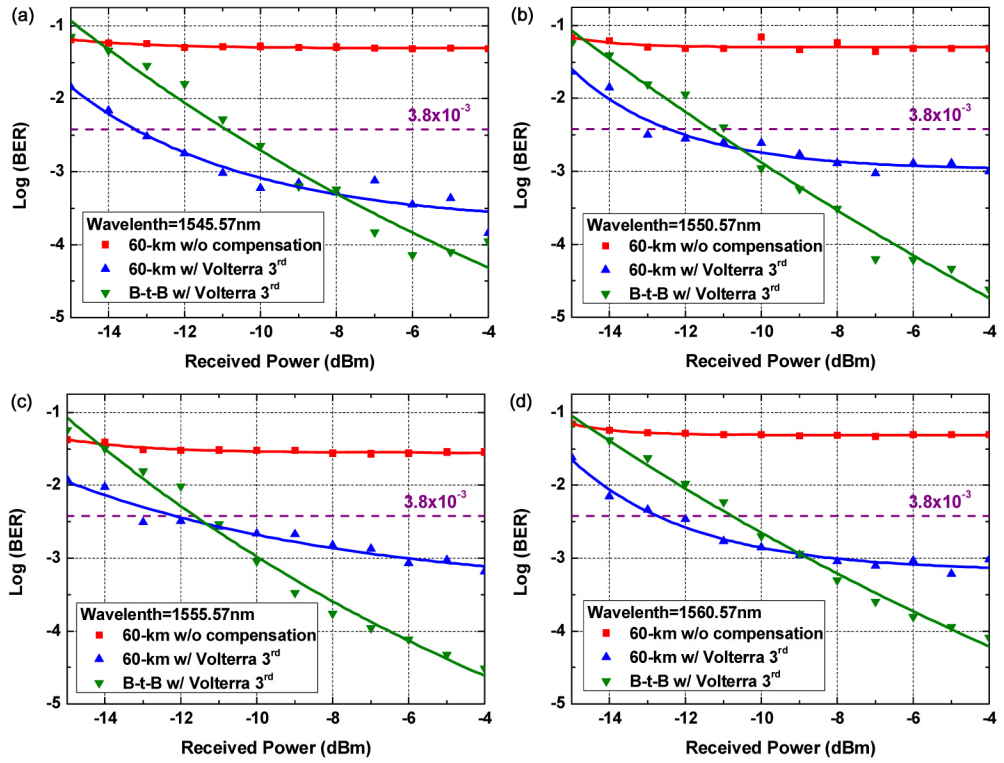

Fig. 12. BER curves of >50-Gbps OFDM signals in co-polarized configuration at wavelengths of (a) 1545.57 nm, (b) 1550.57 nm, (c) 1555.57 nm and (d) 1560.57 nm.

Finally, to investigate the maximum loss budget of a 200-Gbps system using high launch power, we employed 3rd-order Volterra filtering when measuring the BER performance of signals with capacity of >50 Gbps/λ. Four 50-Gbps WDM-OFDM signals were generated using the bit-loading algorithm in accordance with the optimized SNR, based on conditions identical to those shown in Fig. 11, except for the received power of –12 dBm. The data rates for λ_1 to λ_4 were 50.1, 52.6, 51.9, and 50.3 Gbps, respectively. Figures 12(a)–12(d) present the BER curves at each wavelength in back-to-back (B-t-B) and after transmission over a distance of 60 km. Prior to compensation, the BER curves were unable to attain the FEC limit at any of the wavelengths after 60-km SSMF transmission. After compensation, the

Optics EXPRESS

sensitivity values for λ_1 to λ_4 in B-t-B were −10.9, −11.3, −11.6, and −10.8 dBm, respectively. The corresponding sensitivities after 60-km transmission were −13.2, −12.4, −12.2, −12.7 dBm, respectively. Instead of penalty, the signals show improvement in sensitivity after transmission thanks to the SPM-induced power gain. Subtracting the sensitivity values from the fiber launch power resulted in loss budgets of 31.2, 30.4, 30.2 and 30.7 dB. When taking into account the 2-dB loss associated with the 4-channel demultiplexer and 12-dB loss due to 60-km SSMF, each channel is able to support >32 ONUs. Thus, the proposed 128-ONU 60-km system can achieve capacity of >1.6-Gbps/ONU without the need for an inline amplifier or pre-amplifier. These results demonstrate the enormous benefits that can be gained by applying compensation for mixed nonlinear distortion under high fiber launch power, including the elimination of power fading, reduced variation in performance at different wavelengths, high loss budget, and the improvement in sensitivity after fiber transmission.

5. Conclusions

This paper compares the performance of two approaches by which to compensate for nonlinear distortion in an OFDM-IMDD LR systems: SSII cancellation and Volterra filtering. Under normal fiber launch power, power fading and/or significant modulator nonlinearity undermines the effectiveness of 2nd-order Volterra filtering. In contrast, SSII cancellation in the frequency domain is less affected by power fading and higher-order nonlinearity. We also applied high fiber launch power to increase transmission bandwidth and the loss budget. Under high fiber launch power, SSII cancellation was unable to match the performance of 2nd-order Volterra filtering, due to the assumptions pertaining to SPM effects on which it is based. Nevertheless, the distortion compensation provided by both methods proved sufficient to achieve 50-Gbps 60-km OFDM-IMDD transmission with loss budget of >30 dB. Finally, we conducted a comparison of the proposed nonlinear compensation schemes in a 4-channel WDM transmission system. This resulted in a 200-Gbps 60-km OFDM-IMDD system under high launch power. We obtained similar data rates in each channel of the WDM system when 3rd-order Volterra filtering was applied. This resulted in a 200-Gbps 60-km OFDM-IMDD LR transmission, capable of supporting 128 ONUs with capacity of >1.6 Gbps/ONU without the need for an inline amplifier or pre-amplifier.